TRANSVERSE REINFORCEMENT AND DUCTILITY OF REINFORCED CONCRETE HIGH PIER WITH HOLLOW SECTION

Tatsuo OGATA[1], Kumiko SUDA[2] And Junji MASUKAWA[3]

SUMMARY

In order to investigate the seismic performance of reinforced concrete high pier with hollow section, cyclic loading tests were conducted using 15 specimens of 1/10 reduced scale. Reinforcement arrangements of those specimens were very similar to those of real pier. In tests, the effects of following factors were studied: (1)arrangement and amount of transverse reinforcement; (2)range of reinforcement; (3)shape of section at pier bottom; (4)shear span ratio; and (5)torsion. Through this study, it was found that designed ductility could be guaranteed by arranging transverse reinforcement according to the new design code. In addition, structural details of reinforcement arrangement were proposed based on the test results. Finally, measures for predicting ductility and hysteresis damping were developed.

INTRODUCTION

There are numerous plans to construct rigid-frame bridges with high piers over 30 m tall, along expressways such as the Second Tomei Expressway to be built through mountain ranges. Reinforced concrete (RC) high piers usually have hollow sections, in order to reduce their own weight. However, axial compression stress at the bottom of pier is about 3 to 5 N/mm^2, which is over three times higher than that of ordinary piers. In case of rigid-frame structure, torsional force is exerted onto the piers when seismic force perpendicular to the bridge axis causes horizontal deformation of the main girder. Because of relationship between the torsional and bending stiffness, the ratio of torsional moment to bending moment increases as piers become taller. There are many cases where this ratio reached 10 to 20 % at the bottom of piers in elastic response analyses of rigid-frame bridges with high piers. These structural features of high piers are unfavourable from a viewpoint of seismic performance. Thus, it is important to fully understand seismic performance of RC high piers with hollow sections. However, there is no experimental study on the ductility of RC high piers with hollow sections paying special attention to reinforcement arrangement, such as shape or diameter of intermediate ties.

In this study, cyclic loading tests using 1/10 scale models of high piers with various reinforcement arrangements were conducted. Then, effects of transverse reinforcement arrangement on ultimate displacement and hysteresis damping are discussed based on the test results.

OUTLINE OF LOADING TESTS

Here, outline of loading tests using 1/10 scale model of typical high piers designed for highway bridges is described. Typical high piers mean those with a height (H) of 40m, breadth of the cross section (b) of 6m, height of the cross section (h) of 6m, wall thickness (t) of 1m, D51 longitudinal reinforcement placed at a pitch of 150mm, amount of longitudinal reinforcement between 0.02 and 0.03bh, amount of hoops between 0.003 and 0.004ba (a: interval of hoops), and average volumetric ratio of transverse reinforcement between 1 and 1.50%.

[1] *Bridge and Structural Engineering Division, Japan Highway Public Corporation, Tokyo, Japan*
[2] *3-3-2, Kasumigaseki, Chiyoda-ku, Tokyo, 100-0013, Japan E-mail: kohzou4@ho.japan-highway.go.jp*
[3] *Kajima Technical Research Institute, Tokyo, Japan, Fax:+81-424-89-7078*

Specimens

1/10 scale models of typical high piers were prepared for the test (H=3.3 m, b=0.6 m, t=0.1 m, longitudinal reinforcement (D6) placed 27 mm apart, the amount of longitudinal reinforcement of 0.02 bh, the amount of hoops 0.0019 to 0.0063 ba, and average volumetric ratio of transverse reinforcement 0.75 to 2.44 %).

Table 1 shows details of each specimen and reinforcement arrangement. In the tests, the specimen No. 1 was assumed to be a standard specimen. Variations in specimens were related to the following parameters: (i) amount of transverse reinforcement, namely the hoops and ties (Nos. 2, 3, 4, 5, and 16); (ii) patterns of ties (Nos. 6,7, and 8); (iii) diameter of ties (No. 9); (iv) range of reinforcement provided with ties (No. 13); (v) configuration of cross section at the pier base (Nos. 10 and 11); (vi) shear span ratio (No. 12); and (vii) whether torsional force is applied or not (No. 14).

Table 1 Details of Specimens

Specimen No.	Transverse reinforcement								Cross Section at the bottom	Loading	
	Hoops			Intermediate ties						Shear span ratio	Torsion
	Interval (mm)	Type of bars	Amount of hoops	Interval (mm)	Horizontal (mm)	Type of bars	Pattern	Area of Reinforcement			
1	35	D4	0.0036*ba*	35	96	D4	A	Full height	Hollow	5	-
2	30		0.0042*ba*	30							
3	20		0.0063*ba*	20							
4	35		0.0036*ba*	35	187						
5				35	54						
6				70	187		B				
7				35	96		C				
8					98		D				
9					54	D3	A				
10					96	D4			Solid (1*h*)		
11					187						
12					96				Hollow	2.5	
13								1*h*		5	
14								Full height			Present
15	65		0.0019*ba*	65							-

Figure 1 shows a layout of the specimen No.1. For longitudinal and transverse reinforcement, D6 bars and deformed 4-mm and 3-mm bars were used in accordance with the reduction scale of cross sections. The maximum aggregate size was 10 mm. Compression strength of the concrete was between 38 and 42 N/mm^2 and modulus of elasticity between 25 and 29 kN/mm^2, at the time of the test.

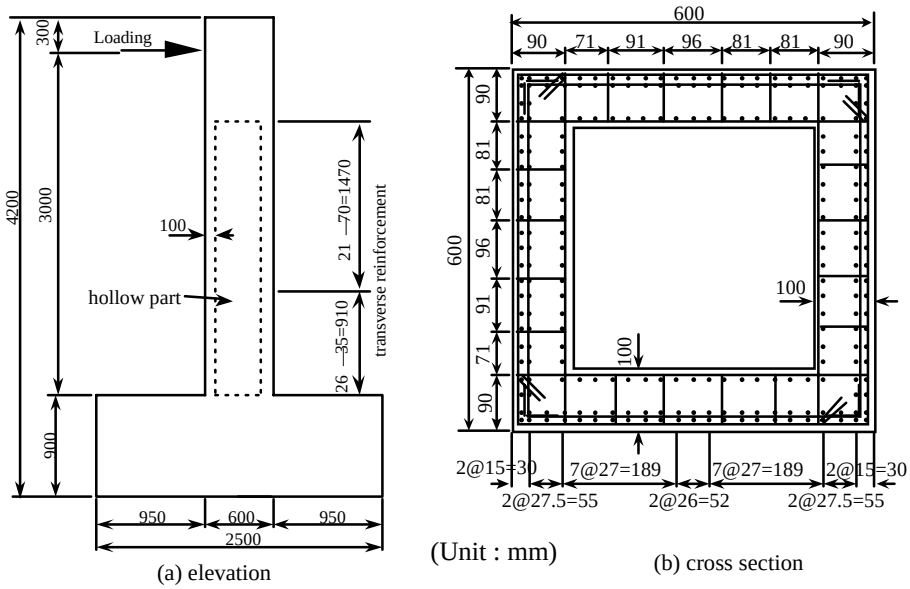

(a) elevation

(Unit : mm)

(b) cross section

Transverse reinforcement was arranged, as shown in Table 1, from the bottom of columns to 1.5 h (900 mm) in all the specimens except for the specimen No.14 which was applied torsional force. Above the height of 1.5 h, interval of transverse reinforcement was doubled.

Patterns of intermediate ties, one of the test parameters, were decided to be four types shown in Figure 2. Type A is a standard pattern where 180º hooks (with an anchorage length of 12 d, where d is the reinforcement diameter) are provided on the outer surface and standard 90º hooks (anchorage length: 12 d) are provided on the inner surface of the cross section, all of which are hooked to the hoops. Type B is a pattern conventionally used for spacing bars, in which both ends are bent as standard 90º hooks (anchorage length: 12 d) and hooked to the longitudinal reinforcement. Type C is a pattern similar to type B, but the ends are hooked to the hoops. Type D is not provided with hooks on the outer ends so enough covering is assured easily, and anchorage length of standard 90º hooks on the inner end is rather short at 5 d. In this test, type D was adopted for the following reasons: because no hooks are provided on the outer end, intermediate ties would still function as transverse reinforcement even when the outer cover concrete is delaminated; and because the ties surround longitudinal reinforcement, it is easier to secure covering by concrete, compared to types A and C where ties are hooked onto the hoops. In the specimens Nos. 10 and 11 with solid cross section at the base, intermediate ties of type A were provided in the solid section, where standard 90º and 180º hooks alternate in a staggered arrangement.

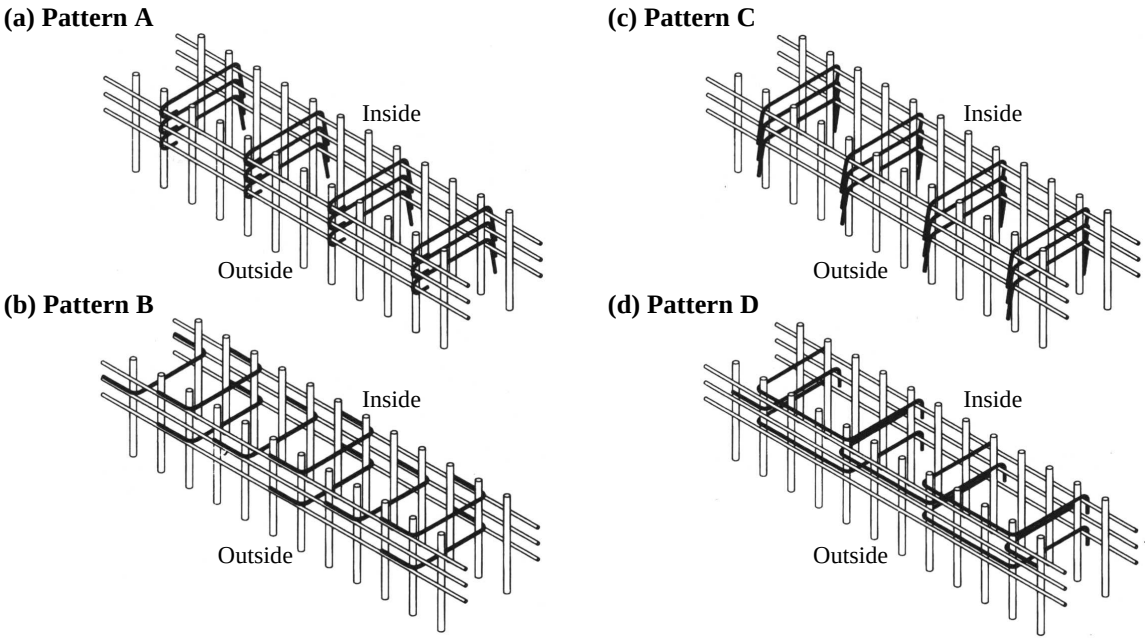

Figure 2 Patterns of intermediate ties

Methods of loading

Cyclic horizontal load and constant axial load was applied to the specimens except for No.14. The axial load was provided by a hydraulic jack mounted on a loading frame via horizontal sliding apparatus, and controlled to maintain a constant value of 588 kN. (The average compression stress in concrete in the hollow sections was 2.94 N/mm^2.) Horizontal loading was controlled based on the value 178.4 kN, which is a design yielding load. Increment of the load was maintained at about 30 kN (for cyclic loading) until design load of yielding was reached; thereafter, displacement was controlled (for cyclic loading of 3 cycles) to be a multiple of the horizontal displacement at design yielding load (the design yield displacement D=11.3 mm).

For the specimen No. 12, the value of D was set at 3.8 mm based on the design yielding load 359 kN, which differs from the rest of the specimens because the shear span ratio of this specimen differs.

To No.14, cyclic horizontal and torsional loads were applied. Torsional loads had been controlled to maintain a constant ratio of 15 % of bending moment at the bottom of column until crack occurred. After crack occurred, loads were controlled to maintain the same ratio between the torsional and bending deformations when crack occurred.

Measurement

Measurements were taken for the loads, displacement, and strain. Cracks were visually inspected. In addition to the horizontal displacement measured at points of loading for the purpose of load control, measurements were also taken for horizontal displacement distribution along columns, average curvature (φ) at the bottom of column, shearing deformation, and torsional angle (for the specimen No.14).

DISCUSSIONS ON THE ULTIMATE DISPLACEMENT

The effect of differences in reinforcement arrangement on the ultimate displacement was studied, based on the test results. Basically, evaluation of the ultimate displacement was calculated following the method indicated in the Specifications for Highway Bridges [Japan Road Association, 1996]. In the Specifications, deformation induced by bending force is calculated based on the M-φ relationship. Here, an attempt was made to introduce a parameter that can reflect differences in the transverse reinforcement arrangement upon the stress-strain relationship of confined concrete. In other words, the ultimate strain of concrete corresponding to the test results was derived by an inverse analysis, and its correlation to the indices pertaining to reinforcement arrangement was studied.

Back analysis on the ultimate strain of confined concrete

Based on the stress-strain relationship of confined concrete in the Specifications, a back analysis on the ultimate strain was performed so that the calculated values and test results (δ_u') for the ultimate displacement would be equal. Figure 3 shows the ultimate strain of confined concrete ε_{cu} obtained by the back analysis. The horizontal axis indicates an index (χ) which incorporates a parameter related to arrangement of transverse reinforcement. The index c is given by Equation (1).

The parameter c is a non-dimensional parameter which is a product of the average volumetric ratio, the ratio

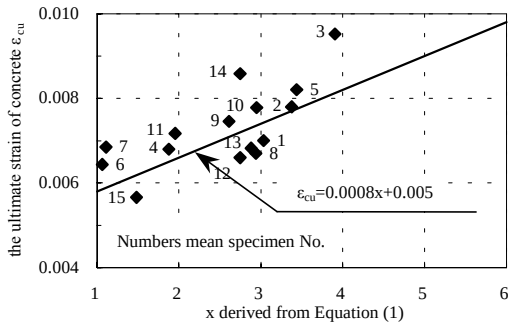

Figure 3 Relationship between ε_{cu} and χ

between the yielding strength of transverse reinforcement and compression strength of concrete, and a parameter indicating degree of restraint of transverse reinforcement.

$$x \quad 100\rho_{sh}\left(\frac{\sigma_{sy}}{\sigma_{ck}}\right)\sqrt{\frac{\frac{d_{tw}}{d_w}}{\frac{l_e}{d_w}-1}} \tag{1}$$

where σ_{sy}: yield strength of transverse reinforcement, σ_{ck}: compression strength of concrete, d_{tu}: diameter of intermediate ties, d_u: diameter of hoops, l_e: effective length of transverse reinforcement

Here, the parameter indicating intensity of restraint of transverse reinforcement was determined taking into consideration that theoretical solution of elastic buckling Pcr can be approximated by Equation (2), and the value of β is governed by the axial stiffness of intermediate ties and bending stiffness of hoops [Suda et al., 1994,1996].

$$P_{cr}, b \quad \sqrt{\beta, d, h} \tag{2}$$

where β: (spring constant of transverse reinforcement) / (intervals between transverse reinforcement), C: a constant, E: apparent modulus of elasticity of steel bars, I: moment of inertia of steel bars

Correlation was observed between the ultimate strain of confined concrete ε_{cu} obtained by a back analysis on the ultimate displacement and the index c, even though the test results fluctuated somewhat. Although a function representing quadratic curve may be appropriate if an example such as the specimen No. 3 is considered, a linear equation shown in Equation (3) is adopted for simplicity to calculate the ultimate displacement of each specimen, which are shown in Figure 4 along with the test results.

$$\varepsilon_{cu} \quad 0.0008x + 0.005 \tag{3}$$

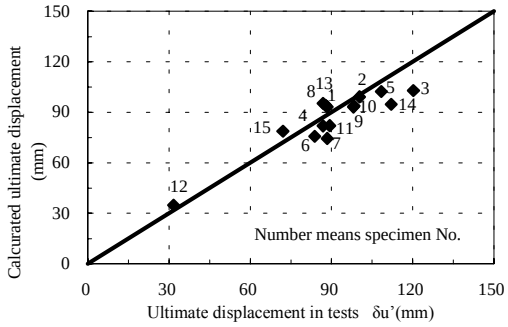

Figure 4 Relationship between test results and the calculated ultimate displacement

The results of calculation for the ultimate strain of confined concrete according to Equation (3) were between 0.84 and 1.10 times the test results for the study, indicating fairly accurate estimation. These results suggest that the index c defined in Equation (1) reflects fairly well the effect of differences in actual arrangement of transverse reinforcement. It should be noted here that Equation (3) is based on the calculation process described in the previous section, and it does not represent material characteristic of confined concrete. In other words, Equation (3) cannot be used if ultimate displacement is derived in a process different from the one described above.

Comparison between the tests results and calculation results according to the Specifications

The ultimate displacement of each specimen was calculated as provided in the Specifications for Highway Bridges [Japan Road Association, 1996], and the results are compared in Figure 5 with the test results. Here, the test results for the ultimate displacement indicated on the horizontal axis show the points where horizontal strength which had been stable in a vicinity of the maximum horizontal strength start falling, as provided in the Specifications for Highway Bridges. In the tests for the study, the displacement correspond to those observed immediately before decrease in the horizontal load by more than 4 % of the maximum horizontal strength. (Note that it is different from δ_u'.) Within the scope of the study, the calculation of the ultimate strain as provided in the Specifications for Highway Bridges yielded values between 0.63 and 1.00 times the test results, which are on the safe side. Since there are limitations imposed on the choice of arrangement of lateral reinforcement, results that

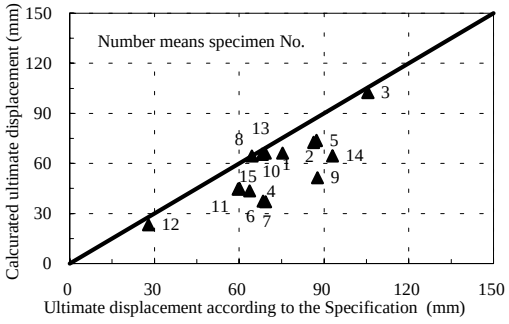

Figure 5 Comparison between tests results and calculation according to the Specifications

are excessively on the safe side were obtained for some of the specimens.

DISCUSSIONS ON THE HYSTERESIS DAMPING

Behavior of bridges with high piers during earthquake is quite complex, so results of non-linear dynamic analysis are often reflected on design. Here, hysteresis model and damping of RC members, which are used for non-linear dynamic analyses, are discussed based on the test results.

Hysteresis models commonly used include those configured by [Muto, 1977] and by [Takeda, Sozen and Nielsen, 1970]. From the view point of unloading stiffness, the model by Muto et al. can be described as origin-oriented, up to the yielding point after cracks start to develop; after yielding, the value decreases due to yielding stiffness, and once a point is reached where bending moment becomes 0, the curve starts rising toward the maximum value in the previous cycle again.

Here, the test results were summarized taking into consideration P-δ relationship of the entire pier and M-θ relationship in the plastic hinge section. At the same time, an attempt was made to develop a formula for calculating unloading stiffness so as to obtain values equivalent to hysteresis damping (equivalent damping factor) derived from the test results, for a case where the method by Muto et al. has been applied for the hysteresis rule except for the unloading stiffness after yielding.

Investigation process

a) Hysteresis damping characteristics of specimens for the model test

Here, P-δ and M-θ relationship, among hysteresis damping characteristics, were investigated. With respect to the P-δ relationship, equivalent damping factor was derived for each hysteresis loop according to Equation (4) (see Figure 6), based on the relationship between horizontal load P and measured horizontal displacement δ at column capital of each specimen.

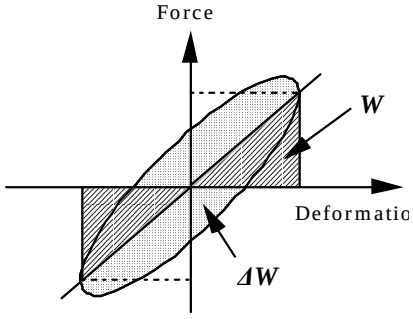

Figure 6 ΔW and W

$$h_{eq} \quad \frac{1}{2\pi} \cdot \frac{\Delta W}{W} \tag{4}$$

With respect to the M-θ relationship, equivalent damping factor was derived for each hysteresis loop as in the case with P-δ relationship, based on the relationship between bending moment M at the base and average curvature φ in the region up to 25 cm (0.42h) from the base, in order to clarify hysteresis damping characteristics in a plastic hinge section. Rotational angle θ of a plastic hinge is expressed as a product of φ and length of the plastic hinge. Here, the length of plastic hinge was assumed to be 25 cm, which is the length of measured region for the average curvature.

b) Investigation on unloading stiffness

Basic hysteresis characteristics, except for unloading stiffness, were assumed to comply with the hysteresis rules according to Muto et al. for the test. By adjusting the values of unloading stiffness, the hysteresis damping characteristics of analysis model were made equivalent with the test results. Specifically, the equivalent damping factor according to the hysteresis rules of Muto et al. is given by Equation (5). Hence, the unloading stiffness k can be expressed as a function of ductility factor μ_r and yielding stiffness k_y.

$$h_{eq} \quad \frac{1}{\pi}\left(1-\frac{k_y}{k}\cdot\frac{1}{\mu_r}\right) \tag{5}$$

Investigation results

Figure 7 shows relationship between the equivalent damping factor derived based on the P-δ relationship and the displacement ductility factor, and Figure 8 shows relationship between the equivalent damping factor derived based on the M-θ relationship and the rotational ductility factor. Here, Model A indicates the relationship derived by a method by [Muto, 1977]. Model B is the modified Model A. Unloading stiffness in Model B is given by Equation (6). Model C indicates the relationship derived by a method by Takeda et al., and Model D is the modified Model C [Takeda, Sozen and Nielsen, 1970].

Within the scope of the study, the hysteresis models yielded results that correspond well with the test results, although in some cases damping was overestimated, especially when ductility factor was small. The models seem sufficiently accurate for practical application. When hysteresis rules by Muto et al. are used, the results would correspond the most with the test results under alternate loading, if unloading stiffness is obtained based on Equation (6), for both P-δ and M-θ relationships.

$$k \quad k_y \cdot \mu_r^{(-0.4)} \tag{6}$$

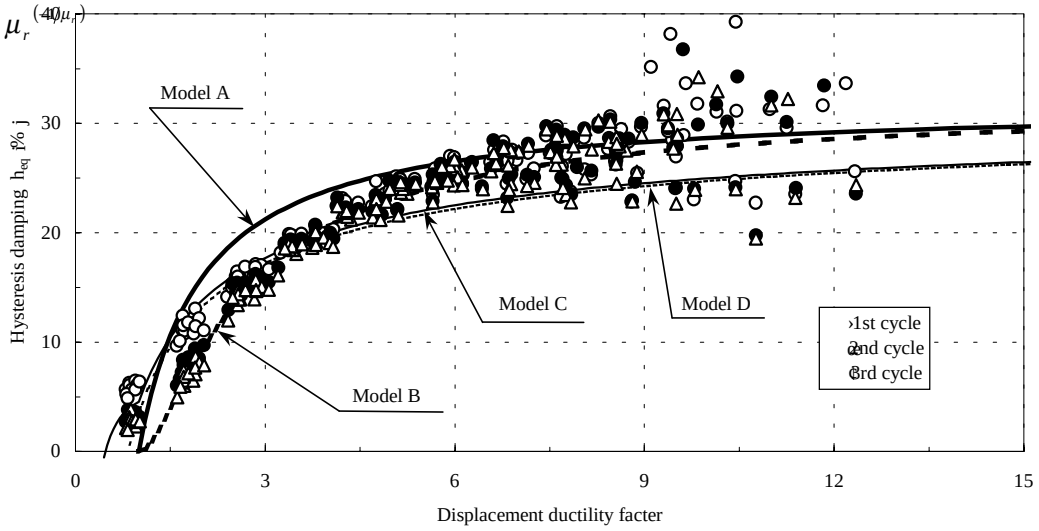

Figure 7 Relationship between h_{eq} derived from P-δ relationship and the displacement ductility factor

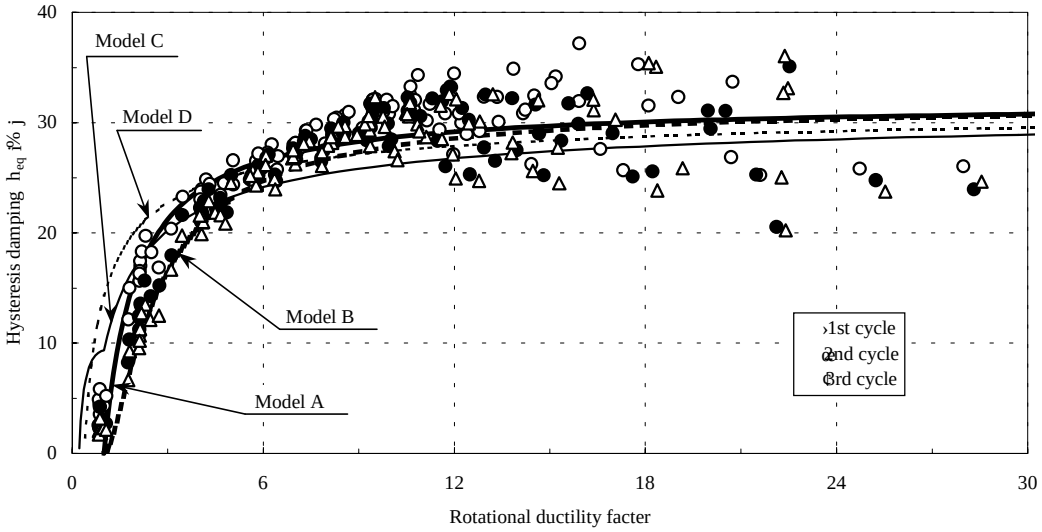

Figure 8 Relationship between h_{eq} derived from M-θ relationship and the rotational ductility factor

PROPOSAL FOR DETAILED SPECIFICATIONS ON REINFORCEMENT

Based on the test results, a proposal is made for detailed specifications on reinforcement for RC high piers with hollow sections. However the model tests for the study were performed under specific conditions, careful consideration should be given under different conditions.

Extent of reinforcement provided with lateral reinforcement

If sufficient shear reinforcement is provided, and failure mode is limited to that induced by bending, rational reinforcement arrangement would be possible by providing intermediate ties at locations where bending failures are likely to occur. To determine the area reinforced with intermediate ties, the area of cover concrete spalling should be considered. In tests, the spalling area was 1/6 h to 1/3 h. The test results indicated that intermediate ties should be provided in regions up to 1 h from the top and bottom ends of piers to be on the safe side, which correspond to three to four times the spalling area.

Patterns and arrangement of intermediate ties

If intermediate ties are arranged in hollow sections as type A, it is better to provide standard 180º hooks on the outer ends and provide standard 90º hooks on the inner ends. Type D arrangement would also exhibit ductility similar to type A arrangement, which is proven as advantageous when it is difficult to secure cover concrete due to limitations imposed by wall thickness, etc. For the type D pattern, anchorage length of standard 90º hooks along the inner surface was set as five times the diameter, which is necessary to secure these hooks onto hoops. In this case, ductility of the specimen proved to be sufficient.

CONCLUSION

The following information was obtained by the tests for RC high piers with hollow sections, in which alternate cyclic loads were applied that assumed seismic load onto models that represent actual piers fairly accurately, with due considerations given for diameters of steel bars and arrangement for reinforcement:

(i) Indices for evaluating effects of arrangement of intermediate ties on ductility was obtained.
(ii) Detail specifications for the reinforcement were proposed, including patterns and arrangement of intermediate ties, their diameters, and methods for reinforcement against torsion.
(iii) After clarifying hysteresis damping characteristics of RC high piers with hollow sections, an equation for evaluating unloading stiffness was proposed, for hysteresis models that represent hysteresis damping characteristics for the tests accurately.

ACKNOWLEDGMENT

The authors are grateful toward the members of the committee on seismic design of bridges with high piers (organized by Expressway Technology Center and chaired by Professor Iemura of Kyoto University), Yasuyuki Yukawa, Tetsuo Matsuda and Yasuo Inokuma of Japan Highway Public Corporation, and many others for their valuable.

REFERENCES

Japan Road Association (1996), *Specifications for Highway Bridges Part V: Seismic Design*, Japan.
Matsuda, T., Yukawa, Y., Yasumatsu, T., Tsukiyama, Y., Ishihara, S., Suda, K., Shimbo, H. and Saito, H.(1996) "Seismic Model Tests of Reinforced Concrete Hollow Piers", *Proc. of 12th US-Japan Bridge Engineering Workshop*, pp407-421.
Muto, K. (1977), *Seismic Design of Structures*, Maruzen, Japan.
Suda, K., Murayama, Y., Ichinomiya,T. and Shimbo, H. (1994), "Buckling Behavior of Longitudinal Reinforcements in RC Column Subjected to Cyclic Load ",*Proc. of JC*I, Vol.16, No.2, pp.467-472.
Suda, K., Shimbo, H., Masukawa, J. and Murayama, Y. (1996), "Reinforcing Method to Improve Ductility of RC Column with Hollow Section ",*Proc. of JCI*, Vol.18, No.2, pp.467-472.
Takeda, T., Sozen, M. A. and Nielsen, N. N. (1970), "Reinforced Concrete Response to Simulated Earthquake", ASCE, Vol.96, No.ST12.